NANO LETTERS

Letter

pubs.acs.org/NanoLett

Edge-on Gating Effect in Molecular Wires

Wai-Yip Lo, Wuguo Bi, Lianwei Li, In Hwan Jung, and Luping Yu*

Department of Chemistry and the James Franck Institute, The University of Chicago, 929 E 57th Street, Chicago, Illinois 60637, United States

Supporting Information

ABSTRACT: This work demonstrates edge-on chemical gating effect in molecular wires utilizing the pyridinoparacyclophane (PC) moiety as the gate. Different substituents with varied electronic demands are attached to the gate to simulate the effect of varying gating voltages similar to that in field-effect transistor (FET). It was observed that the orbital energy level and charge carrier's tunneling barriers can be tuned by changing the gating group from strong electron acceptors to strong electron donors. The single molecule conductance and current−voltage characteristics of this molecular system are truly similar to those expected for an actual single molecular transistor.

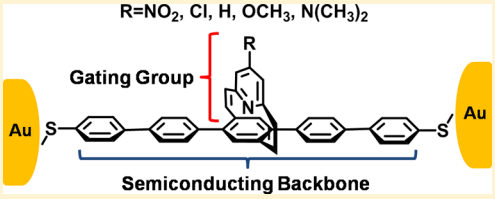

KEYWORDS: *Molecular electronics, STM break-junction, edge-on gating, cyclophane*

Charge transport through single molecules is an active research topic that involves design, syntheses, physical measurements, and theoretical understanding of functional molecules that can control charge transport.[1−3] The extensive research effort in both measurements and theoretical calculations of the charge transport phenomenon has led to deeper understanding on this topic. Different molecular components, including molecular wires and diode molecules were synthesized and investigated. Despite this progress, controlling charge transport through single molecules is still a challenging issue.[4,5] Electric gating is an important means to manipulate charge transport behavior in semiconductor devices, which is the basis of field effect transistors (FET). The same gating effect was pursued in a limited number of field effect transistor structures using single molecular semiconductor, such as C60,[6,7] carbon nanotube,[8] or simple 1,4-benzenedithiol[9] via external third gating electrode separated by an oxide dielectric layer. However, these molecular transistors were prepared with an exhaustive nanofabrication of small electrode gaps with very low yield.[10,11] Other approaches were applied to study the gating effect, such as electrochemical gating.[12−14] There is no molecule that mimics the function of a transistor and can be investigated via a simple approach although several theoretical studies have dealt with this topic.[15,16] An interesting example was reported by Rabeet al., in which the current through a hybride molecular diode is modulated by the formation of charge transfer interaction.[17]

In this study, we have designed and synthesized a single molecular transistor system that contains cyclophane moieties as shown in Figure 1 and investigated their electric gating effect on molecular junctions. The cyclophane moiety (16-aza-tricyclo-[9.2.2.14,8]hexadeca-1(14),2,4,-6,8(16),9,11(15),12-octaene) offers a building motif for transistor molecules containing drain, source, and gating termini; each of them can exhibit orthogonal reactivity for connection to an electric circuit. The building motif is a known compound that was shown to exhibit a perpendicular orientation between two aromatic rings.[18,19] In this molecular

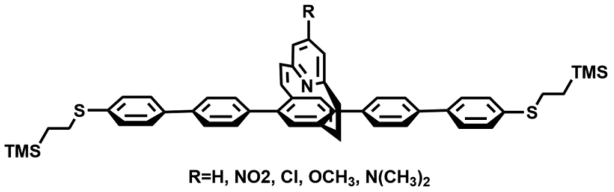

Figure 1. Chemical Structure of the protected cyclophane molecular wires.

system, the perpendicular pyridine moiety is connected to the conjugated semiconducting segment with two vinyl groups. The π-system in the pyridine ring and vinyl groups is orthogonal to that in the semiconducting wire (Figure 1). It provides several covalent bonding sites that can be chemically manipulated to introduce functional groups. This system is designed to mimic the structure of a bulk transistor at the molecular level in which the pyridine unit can be used as the gating end that is not directly conjugated with the semiconducting entity. The double bonds in the cyclophane moiety act as the dielectric component to electrically isolate the gate from the semiconductor. The functional groups exert gating effect indirectly similar to a FET setup. Although our ultimate goal is to connect the molecule to three electrodes via orthogonal reactions, it is currently impossible for us to connect three termini into an external circuit with controlled precision. Thus, we decided first to investigate the chemical gating effect.

Pentaphenylene bearing protected thiols on the ends was chosen to be the molecular semiconductor with structures as shown in Figure 1 in which the cyclophane core is integrated into it with the thiols as the anchoring groups for drain and source electrodes. The edge-on pyridine unit was functionalized with

Received: September 29, 2014
Revised: January 13, 2015

DOI: 10.1021/nl503745b
Nano Lett. XXXX, XXX, XXX−XXX

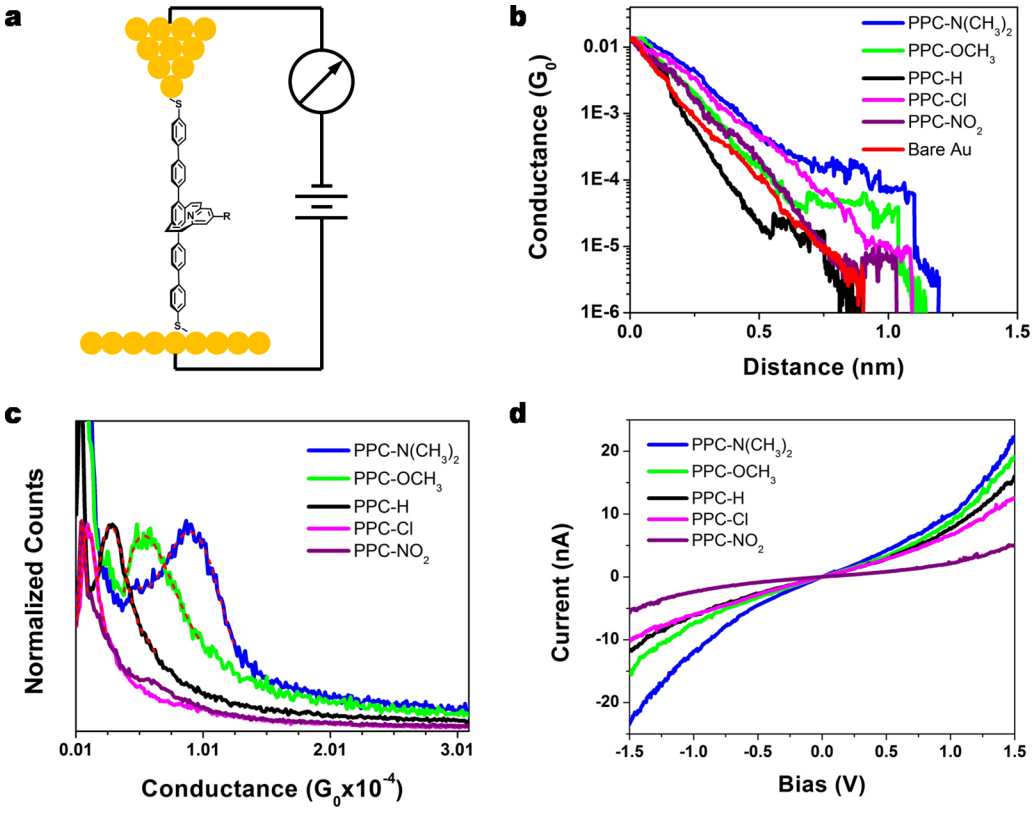

Figure 2. (a) A representative metal−molecule−metal junction in STM break-junction technique. (b) Sample conductance traces of molecular junctions with gating substituent: $-NO_2$, −Cl, −H, $-OCH_3$, and $-N(CH_3)_2$. (c) Conductance histogram of the five molecular junctions. Red dash lines represent polynomial fitting of each peak. (d) Single current−voltage characteristic curves of the five molecular junctions constructed from the average of 30 individual curves.

different groups that possess varied electronic demands, which will play the role of applied gating voltage to modulate the charge conductance in the molecular junction. These substituents, namely NO_2, Cl, H, OCH_3, and $N(CH_3)_2$, are attached onto the para-position of the pyridine in the cyclophane moiety and range from strongly electron withdrawing to strongly electron donating.

To measure the conductance of single molecules, a self-assembled monolayer film of the deprotected molecules was prepared on gold surface via thiol-gold reaction.[20] The molecules with two terminal thiol groups strongly couple with two gold electrodes to form a molecular junction. A representative metal−molecule−metal junction is shown in Figure 2a. The density of the anchored molecules was characterized with cyclic voltammetry after the top thiol group was functionalized with ferrocene thioester as a reporting molecule. It was found that the typical surface coverage of molecules is around 7.2×10^{-10} mol·cm^{-2}. Cyclic voltammogram of the experiment can be found in the Supporting Information.

The conductance of the molecular junctions was measured by using the break-junction technique with a modified STM system.[21−23] The experiments were carried out at 100 mV of bias voltage in toluene according to the protocol by the Tao group.[22] The conductance traces of the molecules with different substituents were recorded by using a LabVIEW program and are shown in Figure 2b. In each measurement, molecule junctions are formed after the gold STM tip was brought into contact with a gold substrate functionalized with a monolayer of compound under a small bias voltage applied between the tip and the substrate. The STM tip was then pulled away from the substrate while monitoring the current between the tip and the substrate. A plateau in the conductance trace, recorded as the current as a function of pulling distance, before junction break would indicate the formation of a single molecule junction (Figure 2b).

The conductance in the last plateau in thousands of current traces for each molecule was analyzed statistically to produce a histogram with a clear peak, which corresponds to the single-molecule conductance at that bias voltage. From the conductance histograms in Figure 2c, the conductance values of molecules PPC-NO_2, PPC-Cl, PPC-H, PPC-OCH_3, and PPC-$N(CH_3)_2$ at 100 mV of bias voltage were determined to be 5.8×10^{-6} G_o, 11×10^{-6} G_o, 2.8×10^{-5} G_o, 5.8×10^{-5} G_o, and 9.1×10^{-5} G_o respectively, where G_o equals $2e^2/h$ (e is the electron charge and h is the Plank constant). Systematic change can be clearly observed when the substituent changes from strong acceptor (NO_2) to strong donor ($N(CH_3)_2$).

To understand the charge transport mechanism in the single molecule junction at an extended bias voltage range, thousands of $I-V$ curves were recorded for each molecule when the STM tip was pinned at the distance corresponding to single-molecule junction, which was deducted from the conductance measurements, and voltage was swept rapidly from −1.5 to 1.5 V. Because of the instability of the single molecular junction caused by various side effects, such as high bias voltages and current-induced heating,[21,24,25] a large portion of $I-V$ curves (e.g., 47% of the total $I-V$ curves for PPC-H) were thrown out automatically by the program.[23]

On the basis of the results of the conductance measurements, $I-V$ curves were measured at the corresponding locations of the plateaus at around 5.8×10^{-6} G_o, 11×10^{-6} G_o, 2.8×10^{-5} G_o, 5.8

DOI: 10.1021/nl503745b
Nano Lett. XXXX, XXX, XXX−XXX

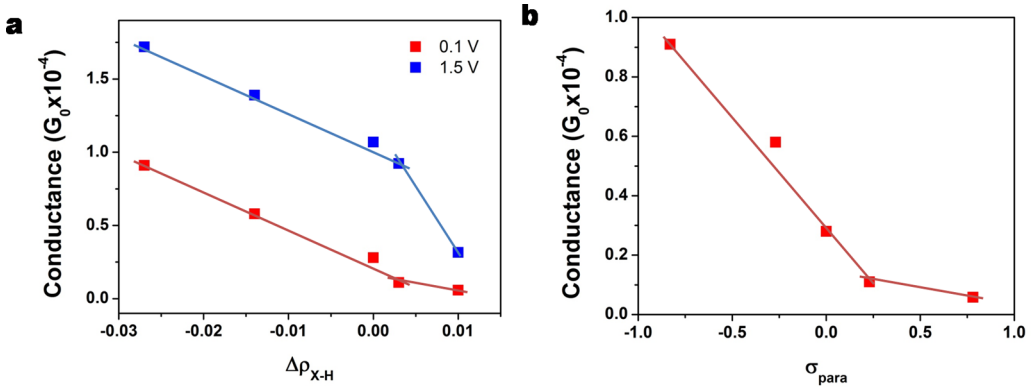

Figure 3. (a) A plot of conductance at 0.1 V (red) and 1.5 V (blue) against difference in charge of the pyridine N (from DFT calculations) of the four substituted PPC compare with PPC-H. The data points from left to right correspond to $-N(CH_3)_2$, $-OCH_3$, $-H$, $-Cl$, and $-NO_2$, respectively. (b) A plot of conductance against Hammet parameters of the corresponding functional group attached at the gate position. Colored lines are only used as eye guide.

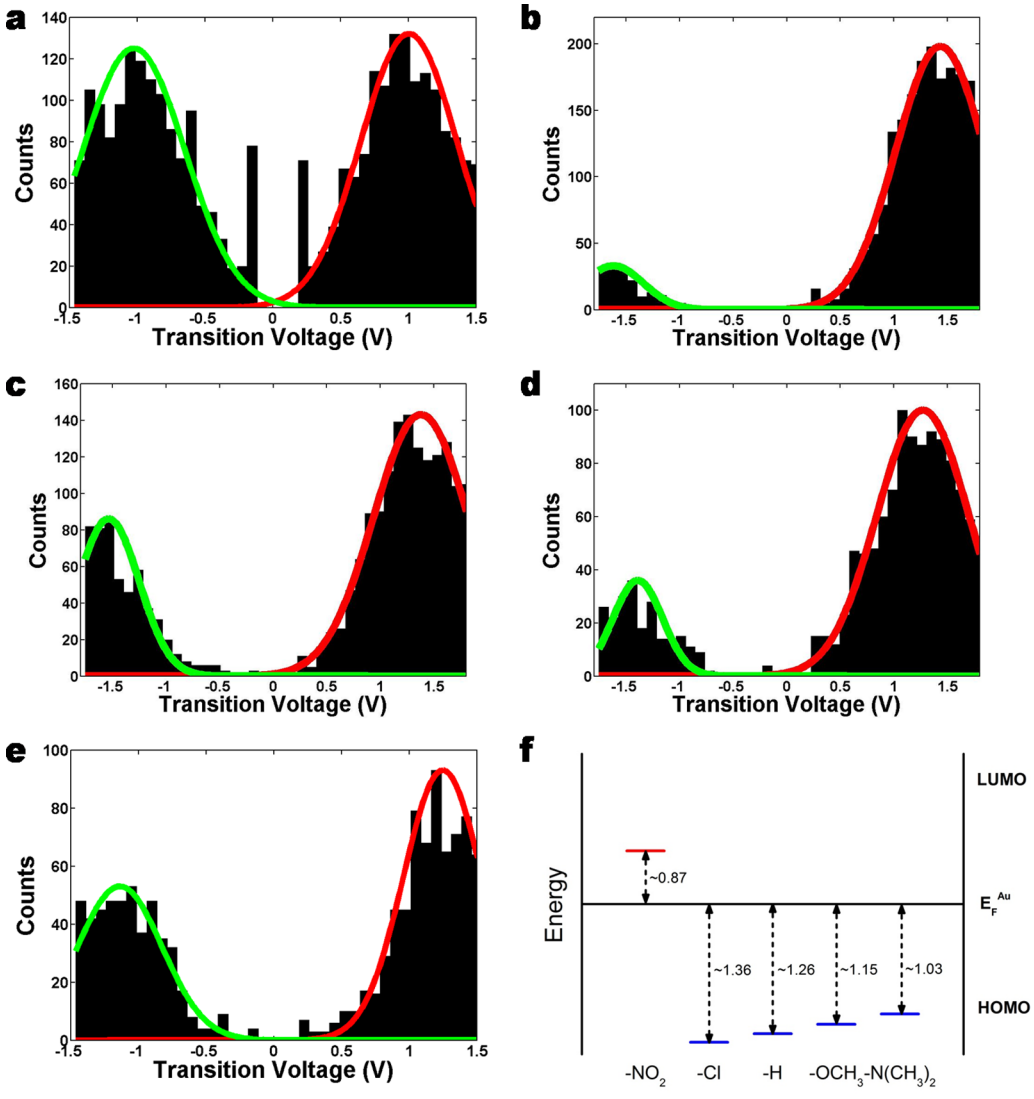

Figure 4. The 1D transition voltage histograms of (a) PPC-NO_2, (b) PPC-Cl, (c) PPC-H, (d) PPC-OCH_3, and (e) PPC-$N(CH_3)_2$ showing the occurrence of transition voltage for each molecular junction. (f) A plot of energy offsets calculated with the transition voltages from panels a−e for all five molecular junctions.

$\times 10^{-5}$ G_o, and 9.1×10^{-5} G_o for PPC-NO_2, PPC-Cl, PPC-H, PPC-OCH_3, and PPC-$N(CH_3)_2$, respectively. The 2D histograms of the $I-V$ and the $G-V$ relations can be found in the Supporting Information. Average $I-V$ curves of the five

DOI: 10.1021/nl503745b
Nano Lett. XXXX, XXX, XXX−XXX

molecular junctions constructed from 30 individual curves are shown in Figure 2d. It can be observed that the current displays a clear nonlinearity as a function of bias voltage. In particular, the current for the molecule with electron donating group increases much faster at higher bias than that with electron withdrawing group. The conductance data clearly showed the gating effect, as the substituent becomes more electron-rich, the conductance increases. A better expression of the gating effect is the interesting correlation of conductance with the charge density change on the nitrogen atom in the pyridine ring. Density functional theory (DFT) calculations of these molecules yield the charge density on each atom. Specifically, we are more interested in the nitrogen atom in the pyridine ring whose charge density was shown in Supporting Information, Table 1. Shown together in the table are also the Hammet parameters σ_{para}, which was developed for characterizing electronic effect of different functional groups on organic reactions. It is interesting to notice that the conductance changes correlate almost linearly with the charge density changes on nitrogen atom of the pyridine ring (relative to −H substituent) except for the compound containing the nitro group (Figure 3a). The Hammet equation gives a similar correlation (Figure 3b). When the pyridine ring in the cyclophane moiety is attached with electron withdrawing group, such as chlorine atom, the electronic density of the pyridine ring is reduced relative to that with hydrogen atom. The nitrogen atom in the pyridine ring bears less negative charge, which is confirmed from quantum mechanics calculation. On the other hand, a donating group ($-N(CH_3)_2$, or $-OCH_3$) can make the pyridine ring, thus the nitrogen atom, more negative, which will facilitate hole current through the molecule and increase the conductance. With no substituent present on the pyridine ring, effectively no bias is applied at the gate. As a comparison, the pentaphenylene wire was also synthesized and their conductance measured. It is very interesting to notice that the pentaphenylenedithiolate molecular junction exhibits a conductance of ca. 7.4×10^{-5} G_o, which is larger that of PPC-H (2.8×10^{-5} G_o), but smaller than that of PPC-NMe_2 (9.1×10^{-5} G_o). The difference is due to the significantly more twisted structure along the conjugating backbone caused by the cyclophane moiety of the PPC molecular wires (i.e., the two phenyl rings next to cyclophane) than the pentaphenylene molecule. The detailed STM break-junction experiment data of the pentaphenylene molecular junction is included in the Supporting Information. Overall, the results indicated that variation in electronic demand in substituent is identical to the change in gating voltage and the single molecular circuit is performing similar to field effect transistor.

To better understand the edge-on gating effect on the charge transport mechanism, transition voltage spectroscopy (TVS) was recorded and used to determine the energy level alignment of the molecule.[26] Each $I-V$ curve was converted into curve of $\ln(I/V^2)$ as a function of $1/V$, theso-called Fowler−Nordheim (FN) plot.[27] The minimum of the FN plot corresponds to the transition voltage V_t and the 1D TVS histograms of the occurrence of the transition voltage can be constructed from these minimum values (Figure 4a−e). The heights of the charge tunneling barriers of molecules can then be deduced from the equation proposed by Baldea based on these transition voltage values.[28] The heights of the tunneling barriers of molecules with substituent groups of $-NO_2$, −Cl, −H, $-OCH_3$, and $-N(CH_3)_2$ was calculated to be ca. 0.87, 1.36, 1.26, 1.15, and 1.03 eV respectively. The results clearly indicated that when the substituent changes from electron donor to electron acceptor, the transition voltage increased, and the charge tunneling barrier increase except for the compound with nitro group. The results of the other four compounds are consistent with the trend in HOMO energy level deduced from DFT calculations by using calculation method RB3LYP with basis set 6-31G* (Supporting Information, Table 1). In particular, the tunneling barrier for nitro group is very interesting and provides insightful information to be discussed below. The TVS histograms also indicated a significant asymmetry of conductance. This effect has been observed in many other systems, both conjugated or nonconjugated, and was attributed to the difference in geometry of two electrodes, one flat surface and the other a sharp tip.[22]

These results indicated that the pyridine unit modulates the conductance of the pentaphenylene via tuning the charge tunneling barriers. Because the main chain of the molecule is a p-type semiconductor, it favors hole transport through the HOMO of the molecule.[29] DFT calculations based on RB3LYP method with basis set 6-31G* show that the HOMO energy level of the molecular wire decreases when the substituent on the pyridine ring change from donor to acceptor (Supporting Information, Table 1). This will cause an increase in charge tunneling barrier assuming the energy level alignment against the Fermi level of the gold was not significantly affected by the substituents. TVS results are consistent with the HOMO energy level changes for Cl, H, OCH_3, and $N(CH_3)_2$ molecules. However, the compound with nitro group exhibited abnormally small tunneling barrier, yet its conductance is lower than other molecules. While studies have shown that the nitro group may potentially interact with gold surface,[30,31] we did not observe any substantial difference between the SAM of the nitro compound and that of the other wire molecules. Conductance histogram of the nitro molecular wire in our experiments shows a single well-defined peak. Interaction from the nitro group with the gold surface would theoretically result in a different conductance value. Cyclovoltametry studies indicated similar surface coverage with other compounds. The similar anchoring effect with molecules containing thiolate and nitro side group was described in literature.[32] The results imply that the conduction mechanism in nitro compound is different from the others. Similar phenomenon can be observed in the effect of substituent on chemical reaction, the linear energy correlation often showed outstanding effect of nitro group due to mechanistic change.[33] From the DFT calculation results, we can notice that the LUMO energy level of the nitro compound (−3.07 eV) is unusually lowered than the others (around $-1.3 \sim -1.6$ eV). On the basis of the tunneling barriers derived from TVS of the other four compounds, the energy offset of the four compounds are shown in Figure 4f, which puts the nitro compound in such energy level alignment that its LUMO energy level is closer to the Fermi energy level of gold electrodes. This implies that the charge transport in nitro compound is actually tunneling through the LUMO orbital. The DFT calculations showed that the LUMO orbital in the nitro compound is almost exclusively confined in the pyridine unit. The charge transport therefore has to tunnel through space via the nitropyridine, leading to diminished conductance.

In conclusion, we have successfully synthesized a molecular wire system that demonstrated for the first time edge-on gating effect by utilizing the pyridinocyclophane moiety as the molecular gate. The gating effect is manifested via tuning the energy levels of the molecular orbitals. Molecular conductance and current−voltage characteristics curves measured via STM break-junction method point out the possibility of molecular switching as a function of gating voltage.

DOI: 10.1021/nl503745b
Nano Lett. XXXX, XXX, XXX−XXX

■ ASSOCIATED CONTENT

Supporting Information

Detailed synthesis; gold substrate, monolayer preparation, and characterizations; STM break-junction experiment; DFT calculated molecular orbitals; and UV−vis/fluorescence spectra. This material is available free of charge via the Internet at http://pubs.acs.org.

■ AUTHOR INFORMATION

Corresponding Author

*E-mail: lupingyu@uchicago.edu.

Notes

The authors declare no competing financial interest.

■ ACKNOWLEDGMENTS

This work was mainly supported by NSF (EAGER-1242729) and partially by NSF (DMR-1263006). This work also benefited from NSF MRSEC at the University of Chicago. The authors thank Professor Nongjian Tao for his generous assistance in training Dr. Wuguo Bi for using break-junction system and providing operating program.

■ REFERENCES

(1) Ratner, M. A. *Nat. Nanotechnol.* **2013**, *8*, 378−381.
(2) Ng, M. K.; Yu, L. P. *Angew. Chem., Int. Ed.* **2002**, *41*, 3598−3601.
(3) Ng, M. K.; Lee, D. C.; Yu, L. P. *J. Am. Chem. Soc.* **2002**, *124*, 11862−11863.
(4) Bernasek, S. L. *Angew. Chem., Int. Ed.* **2012**, *51*, 9737−9738.
(5) Venkataraman, L.; Klare, J. E.; Nuckolls, C.; Hybertsen, M. S.; Steigerwald, M. L. *Nature* **2006**, *442*, 904−907.
(6) Liang, W.; Shores, M. P.; Bockrath, M.; Long, J. R.; Park, H. *Nature* **2002**, *417*, 725−729.
(7) Park, H.; Park, J.; Lim, A. K. L.; Anderson, E. H.; Alivisatos, A. P.; McEuen, P. L. *Nat. Commun.* **2000**, *407*, 57−60.
(8) Martel, R.; Schmidt, T.; Shea, H. R.; Hertel, T.; Avouris, P. *Appl. Phys. Lett.* **1998**, *73*, 2447−2449.
(9) Artes, J. M.; Diez-Perez, I.; Gorostiza, P. *Nano Lett.* **2012**, *12*, 2679−2684.
(10) Song, H.; Kim, Y.; Jang, Y. H.; Jeong, H.; Reed, M. A.; Lee, T. *Nature* **2009**, *462*, 1039−1043.
(11) Baldea, I.; Koppel, H. *Phys. Lett. A* **2012**, *376*, 1472−1476.
(12) Xu, Y. Q.; Fang, C. F.; Cui, B.; Ji, G. M.; Zhai, Y. X.; Liu, D. S. *Appl. Phys. Lett.* **2011**, *99*, 043304.
(13) Olsen, S. T.; Hansen, T.; Mikkelsen, K. V. *Theor. Chem. Acc.* **2011**, *130*, 839−850.
(14) Saha, K. K.; Nikolic, B. K.; Meunier, V.; Lu, W. C.; Bernholc, J. *Phys. Rev. Lett.* **2010**, *105*, 236803.
(15) Mukhopadhyay, S.; Pandey, R. *J. Phys. Chem. C* **2012**, *116*, 4840−4847.
(16) He, H.; Pandey, R.; Karna, S. P. *Nanotechnology* **2008**, *19*, 505203.
(17) Jackel, F.; Watson, M. D.; Mullen, K.; Rabe, J. P. *Phys. Rev. Lett.* **2004**, *92*, 188303.
(18) Weaver, L. H.; Matthews, B. W. *J. Am. Chem. Soc.* **1974**, *96*, 1581−1584.
(19) Boekelheide, V.; Galuszko, K.; Szeto, K. S. *J. Am. Chem. Soc.* **1974**, *96*, 1578−1581.
(20) Whitesides, G. M.; Gorman, C. B. In *Handbook of Surface Imaging and Visualization*; Hubbard, A. T., Ed.; CRC Press: Boca Raton, FL, 1995; p 713.
(21) Diez-Perez, I.; Hihath, J.; Lee, Y.; Yu, L. P.; Adamska, L.; Kozhushner, A.; Oleynik, I. I.; Tao, N. J. *Nat. Chem.* **2009**, *1*, 635−641.
(22) Xu, B.; Tao, N. J. *Science* **2003**, *301*, 1221−1223.
(23) Guo, S. Y.; Hihath, J.; Diez-Perez, I.; Tao, N. J. *J. Am. Chem. Soc.* **2011**, *133*, 19189−19197.
(24) Huang, Z. F.; Chen, F.; D'Agosta, R.; Bennett, P. A.; Di Ventra, M.; Tao, N. J. *Nat. Nanotechnol.* **2007**, *2*, 698−703.
(25) Di Ventra, M.; Pantelides, S. T.; Lang, N. D. *Phys. Rev. Lett.* **2002**, *88*, 046801.
(26) Beebe, J. M.; B, K.; Frisbie, C. D.; Kushmerick, J. G. *ACS Nano* **2008**, *2*, 827−832.
(27) Stern, T. E.; Gossling, B. S.; Fowler, R. H. *Proc. R. Soc. London, Ser. A* **1929**, *124*, 699−723.
(28) Baldea, I. *Phys. Rev. B* **2012**, *85*, 035442.
(29) Reddy, P.; Jang, S.; Segalman, R. A.; Majumdar, A. *Science* **2007**, *315*, 1568−1571.
(30) Venkataraman, L.; Park, Y. S.; Whalley, A. C.; Nuckolls, C.; Hybertsen, M. S.; Steigerwald, M. L. *Nano Lett.* **2007**, *7*, 502−506.
(31) Zotti, L. A.; Kirchner, T.; Cuevas, J.; Pauly, F.; Huhn, T.; Scheer, E.; Erbe, A. *Small* **2010**, *6*, 1529−1535.
(32) Xiao, X.; Nagahara, L. A.; Rawlett, A. M.; Tao, N. *J. Am. Chem. Soc.* **2005**, *127*, 9235−9240.
(33) Hammett, L. P. *Chem. Rev.* **1935**, *17*, 125−136.

DOI: 10.1021/nl503745b
Nano Lett. XXXX, XXX, XXX−XXX